Broadband directional couplers fabricated in bulk glass with high repetition rate femtosecond laser pulses

Wei-Jen Chen, Shane M. Eaton, Haibin Zhang, Peter R. Herman

Edward S. Rogers Department of Electrical and Computer Engineering and Institute for Optical Sciences
University of Toronto, 10 King's College Road, Toronto, ON M5S 3G4 Canada
weijen.chen@utoronto.ca

Abstract: A femtosecond fiber laser was applied to fabricate broadband directional couplers inside bulk glass for general power splitting application in the 1250 to 1650-nm wavelength telecom spectrum. The broadband response was optimized over the 400-nm bandwidth by tailoring the coupling strength and the waveguide interaction length to balance the differing wavelength dependence of the straight interaction and bent transition regions. High spatial finesse of the femtosecond-laser writing technique enabled close placement (~6 μm) of adjacent waveguides that underpinned the wavelength-flattened broadband response at any coupling ratio in the 0% to 100% range. The spectral responses were well-represented by coupled mode theory, permitting simple design and implementation of broadband couplers for bulk 3D optical circuit integration.

OCIS codes: (230.1360) Beam splitters; (250.5300) Photonic integrated circuits; (350.4600) Optical engineering; (230.7370) Waveguides; (350.3390) Laser materials processing; (320.2250) Femtosecond phenomena.

References and links

1. K. M. Davis, K. Miura, N. Sugimoto, and K. Hirao, "Writing waveguides in glass with a femtosecond laser," Opt. Lett. **21**, 1729-1731 (1996).
2. K. Suzuki, V. Sharma, J. G. Fujimoto, E. P. Ippen, and Y. Nasu, "Characterization of symmetric [3 x 3] directional couplers fabricated by direct writing with a femtosecond laser oscillator," Opt. Express **14**, 2335-2343 (2006).
3. A. M. Kowalevicz, V. Sharma, E. P. Ippen, J. G. Fujimoto, and K. Minoshima, "Three-dimensional photonic devices fabricated in glass by use of a femtosecond laser oscillator," Opt. Lett. **30**, 1060-1062 (2005).
4. S. Nolte, M. Will, J. Burghoff, and A. Tuennermann, "Femtosecond waveguide writing: a new avenue to three-dimensional integrated optics," Appl. Phys. A **77**, 109-111 (2003).
5. A. Szameit, F. Dreisow, T. Pertsch, S. Nolte, and A. Tuennermann, "Control of directional evanescent coupling in fs laser written waveguides," Opt. Express **15**, 1579-1587 (2007).
6. H. Zhang, S. M. Eaton, and P. R. Herman, "Single-step writing of Bragg grating waveguides in fused silica with an externally modulated femtosecond fiber laser," Opt. Lett. **32**, 2559-2561 (2007).
7. M. Kamata, M. Obara, R. R. Gattass, L. R. Cerami, and E. Mazur, "Optical vibration sensor fabricated by femtosecond laser micromachining," Appl. Phys. Lett. **87**, 051106 (2005).
8. Y. Sikorski, A. A. Said, P. Bado, R. Maynard, C. Florea, K. A. Winick, C. Inc, and M. I. Dexter, "Optical waveguide amplifier in Nd-doped glass written with near-IR femtosecond laser pulses," Electron. Lett. **36**, 226-227 (2000).
9. R. Osellame, N. Chiodo, G. Della Valle, G. Cerullo, R. Ramponi, P. Laporta, A. Killi, U. Morgner, and O. Svelto, "Waveguide lasers in the C-band fabricated by laser inscription with a compact femtosecond oscillator," IEEE J. Sel. Top. Quantum Electron. **12**, 277-285 (2006).
10. C. M. Lawson, P. M. Kopera, T. Y. Hsu, and V. J. Tekippe, "In-line single-mode wavelength division multiplexer/demultiplexer," Electron. Lett. **20**, 963-964 (1984).
11. C. K. Kirkendall, and A. Dandridge, "Overview of high performance fibre-optic sensing," J. Phys. D: Appl. Phys. **37**, 197-216 (2004).
12. D. B. Mortimore, "Wavelength-flattened fused couplers," Electron. Lett. **21**, 742-743 (1985).

#97770 - $15.00 USD Received 23 Jun 2008; revised 14 Jul 2008; accepted 15 Jul 2008; published 16 Jul 2008

13. A. Takagi, K. Jinguji, and M. Kawachi, "Design and fabrication of broad-band silica-based optical waveguide couplers with asymmetric structure," IEEE J. Quantum Electron. **28**, 848-855 (1992).
14. M. Olivero and M. Svalgaard, "Direct UV-written broadband directional planar waveguide couplers," Opt. Express **13**, 8390-8399 (2005).
15. C. R. Doerr, M. Cappuzzo, E. Chen, A. Wong-Foy, L. Gomez, A. Griffin, and L. Buhl, "Bending of a planar lightwave circuit 2 × 2 directional coupler to desensitize it to wavelength, polarization, and fabrication changes," IEEE Photon. Technol. Lett. **17**, 1211-1213 (2005).
16. K. Jinguji, N. Takato, A. Sugita, and M. Kawachi, "Mach-Zehnder interferometer type optical waveguide coupler with wavelength-flattened coupling ratio," Electron. Lett. **26**, 1326-1327 (1990).
17. A. M. Streltsov and N. F. Borrelli, "Fabrication and analysis of a directional coupler written in glass by nanojoule femtosecond laser pulses," Opt. Lett. **26**, 42-43 (2001).
18. K. Minoshima, A. Kowalevicz, E. Ippen, and J. Fujimoto, "Fabrication of coupled mode photonic devices in glass by nonlinear femtosecond laser materials processing," Opt. Express **10**, 645-652 (2002).
19. S. M. Eaton, W. Chen, L. Zhang, H. Zhang, R. Iyer, J. S. Aitchison, and P. R. Herman, "Telecom-Band Directional Coupler Written With Femtosecond Fiber Laser," IEEE Photon. Technol. Lett. **18**, 2174-2176 (2006).
20. J. D. Love and V. V. Steblina, "Highly broadband buried channel couplers," Electron. Lett. **30**, 1853-1855 (1994).
21. A. Yariv, "Coupled-mode theory for guided-wave optics," IEEE J. Quantum Electron. **9**, 919-933 (1973).
22. R. Syms and J. Cozens, "Coupled mode devices," in *Optical Guided Waves and Devices* (McGraw-Hill International Ltd., 1992), pp. 1-31.
23. F. Ladouceur and J. Love, "Single-mode planar couplers," in *Silica-based Buried Channel Waveguides and Devices* (Chapman & Hall, 1996), pp. 145-162.
24. N. Takato, K. Jinguji, M. Yasu, H. Toba, and M. Kawachi, "Silica-based single-mode waveguides on silicon and their application to guided-wave optical interferometers," J. Lightwave Technol. **6**, 1003-1010 (1988).
25. P. L. Auger and S. Iraj Najafi, "New method to design directional coupler dual wavelength multi/demultiplexer with bends at both extremities," Opt. Commun. **111**, 43-50 (1994).
26. R. Hereth and G. Schiffner, "Broad-band optical directional couplers and polarization splitters," J. Lightwave Technol. **7**, 925-930 (1989).
27. I. Januar and A. R. Mickelson, "Dual-wavelength (λ = 1300-1650 nm) directional coupler multiplexer-demultiplexer by the annealed-proton-exchange process in $LiNbO_3$," Opt. Lett. **18**, 417-419 (1993).
28. S. M. Eaton, H. Zhang, M. L. Ng, J. Li, W.-J. Chen, S. Ho, and P. R. Herman, "Transition from thermal diffusion to heat accumulation in high repetition rate femtosecond laser writing of buried optical waveguides," Opt. Express **16**, 9443-9458 (2008).
29. A. Takagi, K. Jinguji, and M. Kawachi, "Wavelength characteristics of (2×2) optical channel-typedirectional couplers with symmetric or nonsymmetric coupling structures," J. Lightwave Technol. **10**, 735-746 (1992).
30. K. Faerch and M. Svalgaard, "Symmetrical waveguide devices fabricated by direct UV writing," IEEE Photon. Technol. Lett. **14**, 173-175 (2002).
31. P. G. Kazansky, W. Yang, E. Bricchi, J. Bovatsek, A. Arai, Y. Shimotsuma, K. Miura, and K. Hirao, ""Quill" writing with ultrashort light pulses in transparent materials," Appl. Phys. Lett. **90**, 151120 (2007).
32. S. Sowa, W. Watanabe, T. Tamaki, J. Nishii, and K. Itoh, "Symmetric waveguides in poly(methyl methacrylate) fabricated by femtosecond laser pulses," Opt. Express **14**, 291-297 (2006).
33. J. Burghoff, S. Nolte, and A. Tuennermann, "Origins of waveguiding in femtosecond laser-structured $LiNbO_3$," Appl. Phys. A **89**, 127-132 (2007).

1. Introduction

The nonlinear interactions of femtosecond laser light when focused inside transparent glasses offer new promising directions for generating highly functional optical circuits in three dimensional (3D) geometries [1] that are not possible with commercial optical fiber or planar lightwave circuit (PLC) fabrication methods. So far, several groups have reported 3D structures such as 3×3 directional couplers [2, 3], ring resonators [3], 1×3 power splitters [4], and waveguide arrays [5]. Bragg grating waveguides [6], optical sensors [7], waveguide amplifiers [8] and lasers [9] have also been reported. However, there exists a gap in both functionality and performance of devices made by femtosecond laser writing and their commercial counterpart fabricated by traditional methods. In particular, there has been little effort to date in improving the performance and on controlling the spectral response of splitting ratio of directional couplers, a common building block in optical circuits.

Directional couplers typically have strong wavelength dependence due to high modal dispersion and the natural dependence of the interference phenomenon on wavelength. While such dispersion may be attractive for coarse optical filtering such as fiber-to-the-home

#97770 - $15.00 USD Received 23 Jun 2008; revised 14 Jul 2008; accepted 15 Jul 2008; published 16 Jul 2008

wavelength division multiplexing [10], most applications require a flat wavelength response, such as in interferometric sensing [11] and general power splitting. Several approaches have been proposed and demonstrated for flattening the wavelength response of directional couplers, including tapered fiber couplers [12], asymmetric couplers [13, 14], bent couplers [15] and Mach-Zehnder interferometers [16]. However, these designs have not yet been adapted in directional couplers written with femtosecond lasers.

In 2001, the first directional coupler fabricated by femtosecond lasers was reported by Streltsov *et al.* [17] for 633-nm wavelength operation. Minoshima *et al.* extended the study by fabricating a series of directional couplers with varying separation distance and interaction length, demonstrating the expected sinusoidal oscillatory response. However, the maximum cross coupling ratios were significantly less than unity possibly due to imprecise exposure control [18]. In 2006, our group demonstrated zero to near unity power oscillation at both 1310- and 1550-nm wavelengths [19]. Thus far, there have been no attempts to engineer the spectral response of directional coupler.

In this study, we demonstrate broadband power splitters, in both symmetric and asymmetric coupler configuration, written with focused, high-repetition rate femtosecond laser pulses. The broadband responses were observed at small center-to-center separation distances of 6.0 to 7.5 μm, and are interpreted by analyzing the coupling contribution from the straight interaction and the bent transition regions of the directional coupler. It was found that the bent region strongly contributed to the broadband response in contradiction to a number of previous studies where bending effects were neglected [13, 14, 20]. A phenomenological model is presented that accounts for both the straight interaction and bent transition regions through a simple sinusoidal equation. This analysis provides a more comprehensive understanding of broadband couplers and allowed the development of new and insightful design rules for symmetric and asymmetric broadband power splitters. In the field of femtosecond laser writing, this work is the first report of asymmetric couplers, broadband directional coupler devices and presents the first analysis of the bend contribution for aiding coupler design.

2. Coupled mode theory

A directional coupler is composed of two evanescently coupled waveguide arms that typically have a straight interaction region between two bent transition regions. The power splitting ratio depends on interference between the two orthogonal supermodes and their propagation constants along the straight and bent waveguide regions. To simplify modeling, coupled mode theory (CMT) is frequently applied [21-23] in the optical design of directional couplers found in traditional optical fiber and planar lightwave circuits (PLC). CMT works well as long as the waveguide separation is sufficiently large to meet the requirement that one waveguide does not appreciably alter the transverse mode field distribution of the other waveguide. This assumption will be tested for the present laser-fabricated waveguides with center-to-center separation distance as small as 6 μm.

When light of wavelength λ is coupled into waveguide 1, CMT yields the following simple response for the normalized power coupled into waveguide 2:

$$r(\lambda) \equiv \frac{P_2(\lambda)}{P_1(\lambda)+P_2(\lambda)} = \sigma(\lambda)^2 \sin^2\left(\frac{\kappa(\lambda)}{\sigma(\lambda)}L\right) \tag{1}$$

where the amplitude dephasing term is given by

$$\sigma(\lambda) = 1\Big/\sqrt{1+\left(\frac{\Delta\beta(\lambda)}{2\kappa(\lambda)}\right)^2}\,. \tag{2}$$

Here, we define P_1 and P_2 to be the optical power at the output ports of waveguides 1 and 2, respectively. The coupling coefficient, κ, applies to the straight waveguides of length, L, and σ is a dephasing term that reduces the maximum cross coupling ratio according to the degree

#97770 - $15.00 USD Received 23 Jun 2008; revised 14 Jul 2008; accepted 15 Jul 2008; published 16 Jul 2008

of waveguide asymmetry, defined by the difference in propagation constants, $\Delta\beta = |\beta_1 - \beta_2|$, of the two parallel waveguide. The maximum power coupling ratio, σ^2, decreases from unity in the case of symmetric couplers ($\beta_1 = \beta_2$) to fractional values for asymmetric couplers ($\beta_1 \neq \beta_2$), and will be strongly dependent on the wavelength due to the explicit wavelength dependence in $\beta(\lambda) = 2\pi n_{\text{eff}}(\lambda)/\lambda$.

Several studies [16, 24, 25] have identified a significant contribution to the coupler response from the bent waveguide regions, which can be treated phenomenological by adding a bending phase term, $\phi(\lambda)$, to Eq. (1) to yield:

$$r(\lambda) = A(\lambda)\sin^2\left[F(\lambda)L + \phi(\lambda)\right]. \tag{3}$$

To simplify the ensuing discussion, we have substituted $A(\lambda) = \sigma(\lambda)^2$ for the maximum power coupling ratio and $F(\lambda) = \kappa(\lambda)/\sigma(\lambda)$ for the effective coupling coefficient.

To obtain a broadband wavelength-flattened response in symmetric directional couplers, $A(\lambda)$ is unity and only the phase term, $F(\lambda)L + \phi(\lambda)$, must be held constant across the desired wavelength range. Assume $F(\lambda)$ and $\phi(\lambda)$ can be approximated by linear functions, the broadband response is obtained by:

1. Selecting a waveguide separation distance d such that $F(\lambda)$ and $\phi(\lambda)$ have opposite slopes according to $\frac{dF(\lambda)}{d\lambda} < 0$ and $\frac{d\phi(\lambda)}{d\lambda} > 0$.
2. Setting the coupler length to $L = -\frac{d\phi(\lambda)}{d\lambda} \Big/ \frac{dF(\lambda)}{d\lambda}$ to cancel the dispersion between the straight and bent regions of the coupler.

The available bandwidth will be limited by the accuracy of the linear assumption which, in turn, will lead to imperfect dispersion cancellation at step 2.

Symmetric couplers are highly sensitive to imperfect dispersion cancellation around the quadrature phase point in Eq. (3), making broadband response especially difficult around r = 50% (3 dB) splitting ratio. A spectrally flat coupling ratio is therefore better obtained with asymmetric couplers, which can be designed by the following simplified procedures:

1. Start with interaction length $L = 0$ to remove the dispersion of the first phase term $F(\lambda)L$.
2. Select waveguide separation, d, to minimize dispersion in $A(\lambda)$ and $\sin^2(\phi(\lambda))$ terms for an overall wavelength flat response from the two bent waveguide regions.
3. Tune L to adjust the coupling ratio of the final device while keep L small to minimize the impact of the large dispersion in $F(\lambda)$.

Qualitative insight into the above two optimization procedures is found by analyzing the dispersion of $F(\lambda)$ from the case of a symmetric coupler. For light coupling from waveguide 1 to waveguide 2, CMT provides [22]:

$$F(\lambda) = \frac{k_0(\lambda)^2}{2\beta_0(\lambda)} \iint_{A_2} (n_2(x,y,\lambda)^2 - n(\lambda)^2) u_1(x,y,\lambda) u_2(x,y,\lambda) dA, \tag{4}$$

where the integration is carried out over A_2, the cross section of waveguide 2. β_0 is the propagation constant of individual waveguides in isolation, n_2 is the refractive index profile in waveguide 2, n is the bulk medium refractive index, and u_1 and u_2 are the normalized unperturbed electric field distribution for waveguides 1 and 2, respectively. The wavelength dependence in $F(\lambda)$ has four components of wavelength dispersion:

1. The $k_0^2/2\beta_0$ term decreases with increasing wavelength roughly as a function of $1/\lambda$ [22].
2. u_1 increases with increasing wavelength due to weaker mode confinement leading to a stronger evanescent tail overlapping with waveguide 2.
3. u_2 decreases with increasing wavelength since less light is guided in the core of waveguide 2 due to weaker mode confinement.
4. The material dispersion introduced by $n_2(\lambda)$ and $n(\lambda)$ typically give negligible contribution to the overall dispersion of $F(\lambda)$.

#97770 - $15.00 USD Received 23 Jun 2008; revised 14 Jul 2008; accepted 15 Jul 2008; published 16 Jul 2008

Equation (4) thus yields a response of $F(\lambda)$ that may increase or decrease depending on the contribution from the above four components.

Hereth *et al*. [26] computed the net effect of the above contributions in twin-core fiber couplers and showed $F(\lambda)$ to increase monotonically with increasing wavelength for larger separations distances (>15 μm). This increasing response is often assumed in directional coupler design, but the trend reverses as d decreases, and leads to a coupling coefficient with a peak value inside the design spectral window. The peak value shifts to a shorter wavelength as waveguide separation distance decreases, and eventually $F(\lambda)$ will have a negative slope across the full design wavelength window, providing the desired condition to compensate for the positive slope in the bending phase $\phi(\lambda)$. Bending phase is given by twice the integral of the coupling coefficient over the length of one S-bend [27]:

$$\phi(\lambda) = 2\int F(z,\lambda)dz\,. \tag{5}$$

Based on this equation, bending phase will take on a similar character as the coupling coefficient except that the average separation distance is larger than that for the straight region. There is therefore a range of separation distance where $F(\lambda)$ is negatively sloped and $\phi(\lambda)$ is positively sloped, ideal for broadband symmetric couplers. At even smaller d, $F(\lambda)$ becomes negatively sloped, and $\phi(\lambda)$ nearly flatten, which is ideal for asymmetric broadband couplers. In this case, a zero or very small interaction length is preferred (i.e. $F(\lambda)L \approx 0$). These principles for designing broadband directional couplers will be tested for ultrashort-pulse laser-written waveguides.

3. Experiments

Directional couplers were fabricated with a commercial femtosecond fiber laser (IMRA America μJewel D-400-VR) having 1045-nm center wavelength, 300-fs pulse duration, 1.5-MHz repetition rate, and 200-mW average power [28]. Boroaluminosilicate glass samples (Corning EAGLE2000) of 50-mm length were translated transversely on precise *xy* air-bearing motion stages (Aerotech ABL1000) at speeds of 8 to 20 mm/s with laser polarization perpendicular to the sample motion. The laser beam was focused with a 0.55-NA aspherical lens to ~2-μm diameter ($1/e^2$ of intensity) spot size at 150 μm below the sample surface.

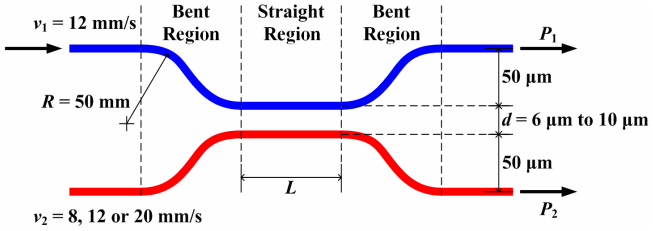

Fig. 1. Schematic of a directional coupler consisting of two waveguide arms written by a femtosecond laser. See text for definitions.

Figure 1 shows the layout of directional couplers used for both uniformly symmetric and uniformly asymmetric couplers as defined by the nomenclature of Takagi *et al*. [29]. A scan speed of v_1 = 12 mm/s was selected to form the first arm and the second arm was scanned at a speeds of v_2 = 12 mm/s for symmetric couplers, and 8 and 20 mm/s for asymmetric couplers. In the bent transition regions, double S-bends were selected with 50-mm radius of curvature to minimize waveguide bending loss [19]. The center-to-center separation distance of the waveguide arms in the straight interaction region was varied from d = 6 to 10 μm to test various coupling strengths while interaction length L was varied in 0.5-mm steps from L = 0 to 2.5 mm to sample the sinusoidal oscillation.

Light was launched into the couplers from butt-coupling fibers with index matching oil applied between the fibers and end facet. The guided modes were imaged by a 60×

#97770 - $15.00 USD Received 23 Jun 2008; revised 14 Jul 2008; accepted 15 Jul 2008; published 16 Jul 2008

magnification objective to a phosphor-coated CCD camera (Spiricon SP-1550M). A tunable laser (Photonetics Tunics-BT) was used to assess insertion loss and mode profiles at 1550-nm wavelength and a broadband light source (Agilent 83437A) was employed to measure spectral responses from 1250 to 1650-nm wavelength. The fiber-coupled output was collected via a power detector (Newport 818-IG) or optical spectrum analyzer (Ando AQ6317B).

4. Results

4.1 Waveguides

An extensive waveguide writing study revealed an optimum propagation loss of ~0.35 dB/cm at laser repetition rate of 1.5 MHz, average power (pulse energy) of 200 mW (133 nJ), and scan speed range of 8 to 20 mm/s [28]. The mode profiles, mode field diameter (MFD) ($1/e^2$ value of Gaussian fit of intensity profile) and insertion loss (IL) at 1550-nm wavelength are shown in Fig. 2 for the different scan speeds. The waveguide MFD increased from 8.5 to 11.2 μm as the fabrication speed increased from 8 to 20 mm/s, providing a convenient mean for introducing the $\Delta\beta$ mismatch in the waveguides required in the asymmetric couplers.

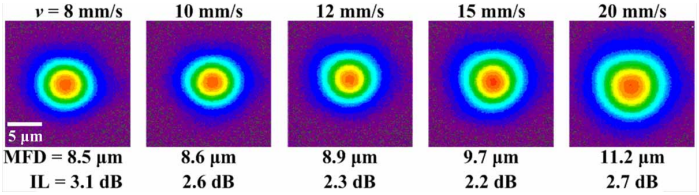

Fig. 2. Near-field mode profiles, MFD and IL measured at 1550-nm wavelength for waveguides formed at scan speeds of v = 8, 10, 12, 15 and 20 mm/s. Scale shown applies to all mode profiles.

4.2 Symmetric directional couplers

The measured coupling ratio for symmetric couplers is plotted against wavelength in Fig. 3 for d = 6-μm waveguide spacing and interaction lengths of L = 0.0, 0.5, 1.0, 1.5, 2.0, and 2.5 mm. A large wavelength range of 1250 nm to 1650 nm was examined, covering all telecommunication bands. Near unity coupling with coupling ratio r = 97.9% ± 2.0% was observed over the full 400-nm bandwidth for L = 1 mm, deviating from the usual sinusoidal wavelength modulation [29] due to the balanced and opposing dispersion in the $F(\lambda)L$ and $\phi(\lambda)$ terms in Eq. (3). This broadband condition is most easily met at the '0' and '1' extrema of the sinusoidal function, limiting broadband operation to power splitting ratios of r = 0~10% and 90~100%, respectively. Otherwise, as Fig. 3 shows, increasing interaction lengths L > 1 mm, lead to less flat spectral responses, eventually developing into sinusoidal wavelength dependence that is most apparent in the wider gapped (d = 10 μm) couplers (data not presented). However, for applications that do not require large bandwidth, one can also find useful 100-nm wide windows such as the r = 40.0%±0.7% and 25.7%±1.4% coupling ratios identified by horizontal arrows in Fig. 3.

#97770 - $15.00 USD Received 23 Jun 2008; revised 14 Jul 2008; accepted 15 Jul 2008; published 16 Jul 2008

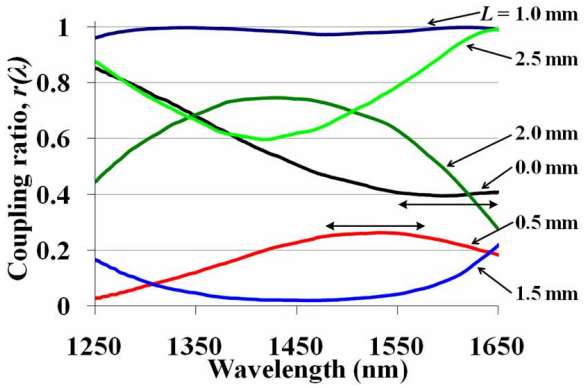

Fig. 3. Measured coupling ratio versus wavelength for symmetric directional couplers with separation distance d = 6 μm and interaction lengths L = 0, 0.5, 1, 1.5, 2, and 2.5 mm.

The highest peak coupling ratio obtained for symmetric couplers was r = 99.8%, which setting to $A(\lambda)$ = 99.8% in Eq. (3) yields $\Delta\beta$ = 0.202 rad/mm for the propagation mismatch in two waveguide arms. This small $\Delta\beta$ value underscores the finesse of the present high-repetition rate femtosecond-laser writing process in constructing two identical waveguides in such close proximity (d = 6 μm) without saturation, degradation or collateral damage. This contrasts strongly with direct UV laser writing, where saturation in photosensivity response contributed to a significant propagation constant offset of closely spaced waveguides and prevented the formation of symmetric couplers [30]. Symmetric waveguides with 6-μm center-to-center separation were not anticipated given the strong heat accumulation effect found at 1.5 MHz repetition rate [28], which positions the guiding core (~2 μm diameter) of the second waveguide entirely within the large 12-μm diameter of the heat-modified cladding of the first waveguide. Furthermore, the two waveguide arms were scanned in opposite directions, suggesting that the directional dependence of waveguide formation, noted as the 'quill effect" [31], is negligible (i.e. $\Delta\beta \approx 0$) for the exposure conditions used here.

The spectral responses for $F(\lambda)$ and $\phi(\lambda)$ were determined by fitting the coupling ratio data of Fig. 3 at each wavelength to the sinusoidal response expected in Eq. (3) for varying interaction length L. Figure 4 shows an example of measured coupling ratio data versus L at 1310-nm and 1550-nm wavelengths together with their calculated representations. The data accurately followed sinusoidal responses with average root mean square (RMS) error of 1.4% across all wavelength data points. The accurate data representation clearly demonstrates the validity of coupled mode theory (Eq. (3)) for femtosecond laser written waveguides, even for the close 6-μm waveguide separation.

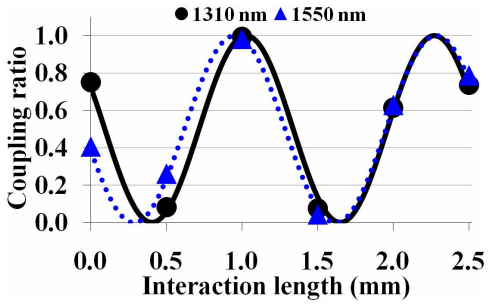

Fig. 4. The coupling ratio versus interaction length at 1310-nm (black) and 1550-nm (blue) wavelength for symmetric coupling at d = 6-μm separation. The lines are the least-squares-error sinusoidal curve representations of Eq. (3).

#97770 - $15.00 USD Received 23 Jun 2008; revised 14 Jul 2008; accepted 15 Jul 2008; published 16 Jul 2008

The extracted values for coupling coefficient $F(\lambda)$ and bending phase $\phi(\lambda)$ are presented in Fig. 5 for waveguide separations of d = 6, 6.5, 7.5 and 10 μm. Due to the small propagation constant offset found above, $F(\lambda) \approx \kappa(\lambda)$ is a good approximation for these symmetric couplers. Both the coupling coefficient and bending phase terms decrease strongly with increasing waveguide spacing d due to the rapidly decreasing overlap of the u_1 and u_2 in Eq. (4). For 10-μm separation distance, both the coupling coefficient and bending phase are positively sloped, preventing a wavelength-flattened response regardless of the choice of interaction length, L. These directional couplers provide sinusoidal wavelength response that might be attractive for coarse wavelength multiplexing application [27]. In Fig. 5, as the waveguide separation distance decreases, the coupling coefficient forms a maximum value that shifts to a shorter wavelength with $\kappa(\lambda)$ transitioning from a positive to a negative slope. These trends are delayed for the bending phase, which retains a positive slope for most of the data range in agreement with the modeling by Hereth *et al.* for the twin-core fiber coupler [26] and the trends discussed above for Eq. (5). This trend is attractive for generating a broadband wavelength-flattened coupling response through suitable choice of interaction length, L, for each separation distance. The offsetting slope condition is best satisfied at 6-μm separation, producing the broadest flat-wavelength response at L = 1 mm (r = 97.9% ± 2.0%) as shown in Fig. 3. Further reduction in separation distance resulted in poor sinusoidal representation of $r(\lambda)$ data by Eq. (3), indicating a breakdown of the weak coupling assumption in CMT.

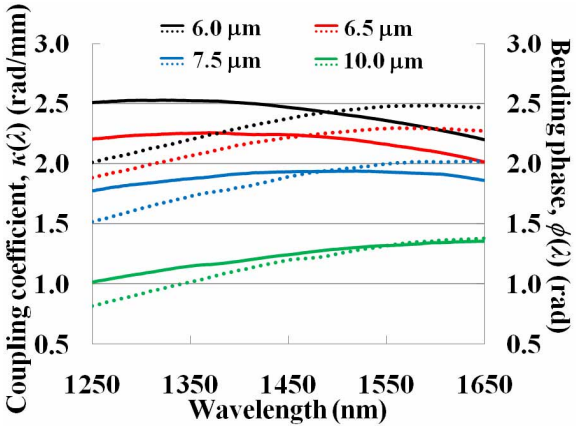

Fig. 5. Coupling coefficient (solid lines) and extra phase (dashed lines) versus wavelength for symmetric couplers with separation distances of d = 6, 6.5, 7.5 and 10 μm.

4.3 Asymmetric directional couplers

To achieve flatter responses compared with the symmetric coupler case, particularly near 50% splitting ratio, asymmetric directional couplers were fabricated. The measured coupling ratio for asymmetric couplers (v_2 = 20 mm/s) is plotted from 1250- to 1650-nm wavelength in Fig. 7 for d = 7.5-μm separation distance and L = 0.0, 0.5, 1.0, 1.5, 2.0, and 2.5-mm interaction length. Flat spectral responses are observed for the shortest interaction lengths of L = 0 and 0.5 mm. The dispersion in $F(\lambda)$ is amplified at longer interaction length, rapidly narrowing the bandwidth for wavelength-flattened coupling.

#97770 - $15.00 USD Received 23 Jun 2008; revised 14 Jul 2008; accepted 15 Jul 2008; published 16 Jul 2008

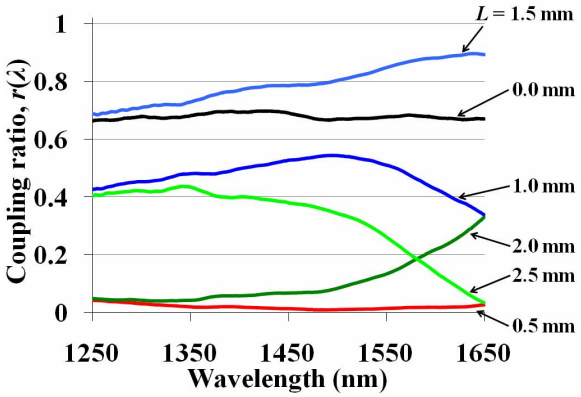

Fig. 6. Measured coupling ratio versus wavelength for asymmetric directional couplers with separation distance d = 7.5 μm, second arm scan speed of v_2 = 20 mm/s and interaction lengths L = 0, 0.5, 1, 1.5, 2, and 2.5 mm.

Using a similar calculation routine as the symmetric coupler, spectral responses of $A(\lambda)$, $F(\lambda)$ and $\phi(\lambda)$ were determined for the asymmetric couplers by using Eq. (3) to represent the measured power coupling ratio as a function of the interaction length, L. Figure 7 shows an example of sinusoidal representations for 1310-nm and 1550-nm wavelength coupling ratio in an asymmetric coupler fabricated with v_1 = 12 mm/s, v_2 = 20 mm/s and d = 7.5 μm. The peak coupling ratios are 0.789 and 0.897 at 1310 and 1550 nm, respectively, clearly demonstrating the wavelength dependence in $A(\lambda)$. The coupling responses for the asymmetric couplers showed an average RMS fitting error of only 0.5%.

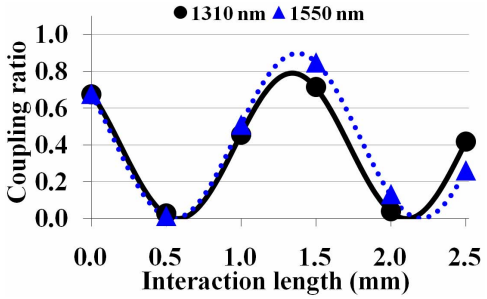

Fig. 7. The coupling ratio versus interaction length at 1310-nm (black) and 1550-nm (blue) wavelength for asymmetric coupling at d = 7.5-μm separation. The lines are the least-squares-error sinusoidal curve representations of Eq. (3).

The experimental values for $F(\lambda)$ (solid lines) and $\phi(\lambda)$ (dotted lines) for asymmetric couplers with separation distances of d = 6, 6.5, 7, 7.5 and 10 μm are plotted in Fig. 8(a). Similar to the symmetric coupler case (Fig. 5), both $F(\lambda)$ and $\phi(\lambda)$ increase as the separation decreases due to stronger evanescent coupling. At the largest 10-μm separation, $F(\lambda)$ is nearly flat, and the $\phi(\lambda)$ function is positively sloped. However, this separation distance is not ideal for wavelength flattened response due to the strong dispersion (slope) in $\phi(\lambda)$. Decreasing the separation distance (d = 7.5, 7.0, 6.5, and 6.0 μm) leads to a flatter $\phi(\lambda)$ responses while $F(\lambda)$ becomes more negatively sloped. Note that this particular operating regime ($\phi(\lambda)$ flat and $F(\lambda)$ negatively sloped) was not observed in the symmetric coupling case in Fig. 5. From the design guideline in Section 2, the asymmetric coupler optimization objective is to reduce the dispersion effect in $F(\lambda)$ by simply selecting short interaction distance L.

#97770 - $15.00 USD Received 23 Jun 2008; revised 14 Jul 2008; accepted 15 Jul 2008; published 16 Jul 2008

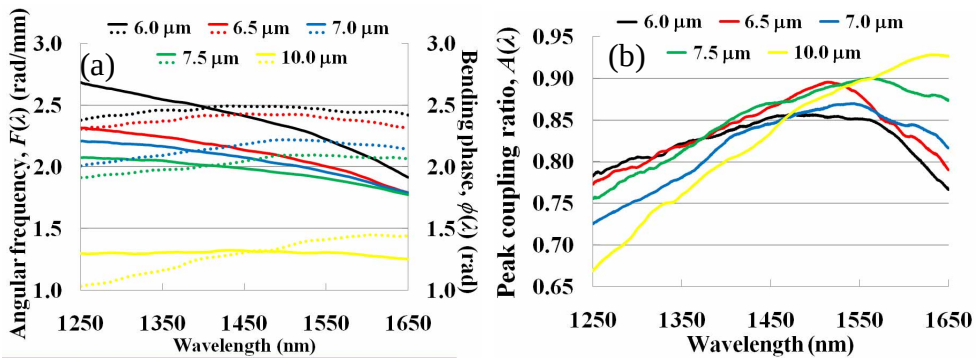

Fig. 8. (a) Measured values of effective coupling coefficient $F(\lambda)$ (solid lines) and bending phase $\phi(\lambda)$ (dotted lines) together with (b) peak coupling ratio $A(\lambda)$ for asymmetric directional couplers (v_2 = 20 mm/s) at a waveguide separation distance of d = 7.5 μm.

Data representations as in Fig. 7 also provided the spectral responses for the peak coupling ratio, $A(\lambda)$, plotted in Fig. 8(b). Following the design guideline in Section 2 for wavelength-flattened asymmetric couplers, we seek only the minimally dispersive $A(\lambda)$ cases to balance with the nearly flat $\phi(\lambda)$ responses in Fig. 8(a). The $A(\lambda)$ dispersion is strongest at a separation d = 10 μm, varying from 66.9% to 92.8% for a maximum-to-minimum coupling ratio variation of 25.9%. The response range decreased from 25.9% to 9.1% as the separation distance d was reduced from 10.0 to 6.0 μm. Clearly, it is more desirable to operate at a small separation distances (d < 10 μm) where both $A(\lambda)$ and $\phi(\lambda)$ are simultaneously wavelength-flattened, and with very small interaction lengths to avoid dispersion in $F(\lambda)$, but tuned to the desired final coupling ratio.

4.3 Broadband directional couplers

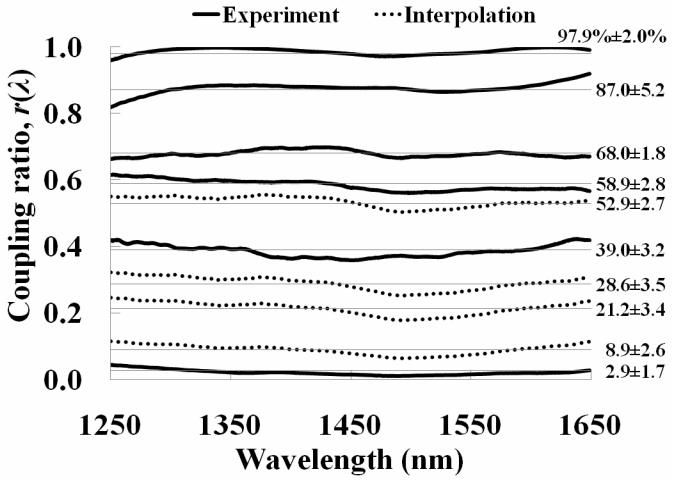

Fig. 9. Measured and interpolated responses of directional couplers with coupling ratios of r = 0, 10, 20, 35, 50, 60, 70, 90 and 100% based on design parameters in Table 1. Coupling ratio and flatness deviation are shown to the right of each graph.

The flattest broadband coupler responses found in this study are shown as solid lines in Fig. 9 with the coupling ratio and flatness variation indicated on the right. The dashed lines represent data at interpolated interaction lengths based on Eq. (3) and the measured $A(\lambda)$, $F(\lambda)$ and $\phi(\lambda)$ data (Fig. 8). The corresponding coupler geometries and device specifications are shown in Table 1 with the interpolated data highlighted. The device providing the broadest 3-dB power

#97770 - $15.00 USD Received 23 Jun 2008; revised 14 Jul 2008; accepted 15 Jul 2008; published 16 Jul 2008

ratio was an asymmetric coupler formed with v_1 = 12 mm/s, v_2 = 20 mm/s scan speeds, d = 7 μm waveguide separation and L = 0 mm interaction length, yielding r = 58.9% ± 2.8% over the 400-nm wavelength window. By interpolating between interaction lengths, we predict that an aysmmetric coupler with r = 52.9% ± 2.7% can be fabricated with v_1 = 12 mm/s, v_2 = 20 mm/s, d = 7.5 μm and L = 0.1 mm.

Table 1. Broadband directional couplers: design and performance (v_1 = 12 mm/s)

***r* (%)**	2.6	8.9	21.2	28.6	39.0	52.9	58.9	68.0	87.0	97.9
±Δ*r* (%)	1.7	2.6	3.4	3.5	3.2	2.7	2.8	1.8	5.2	2.0
v*$_2$ *(mm/s)	20	20	20	20	20	20	20	20	8	12
***d* (μm)**	7.5	7.5	7.5	7.5	6.5	7.5	7	7.5	6	6
***L* (mm)**	0.5	0.4	0.3	0.25	0	0.1	0	0	1	1

The bandwidth and spectral flatness of the selected power splitters in Table 1 are comparable with wavelength-flattened directional couplers made in PLCs by photolithography and direct UV laser writing [13-15]. However, the femtosecond laser writing technique applied in this study presents a number of advantages over several existing fabrication technologies. Fused fiber technology is not suitable for large scale and compact integration, while photolithography requires expensive clean room technology and is not ideal for fast prototyping or manufacturing of custom components. In comparison to direct UV writing, femtosecond laser writing offers 10-fold faster writing speeds and strong photosensitive responses without any photosensitization procedures [14]. In addition, femtosecond laser writing is applicable to a wide variety of material substrates including active-doped glass [8], polymers [32] and crystals [33]. Femtosecond laser writing also offers the unique ability to write full 3D optical circuits. The disadvantages are the relatively higher propagation loss (~0.35 dB/cm [28]) and limited refractive index contrast (Δn ~ 0.01 [28]), but these may improve with further process optimization.

5. Conclusion

Symmetric and asymmetric directional couplers formed by femtosecond laser direct writing were optimized for broadband responses in 1250 to 1650-nm wavelength window. In the case of symmetric couplers, the flattened response was obtained by compensating the wavelength dispersion between the straight and bent region of a directional coupler. On the other hand, asymmetric broadband couplers were optimized for power splitting ratios in the 2.6% to 87.0% range by minimizing the dispersion in the bent region and using short interaction length. An empirical design approach based on CMT was outlined which improves upon existing methodologies [13, 14] by taking into account the evanescent coupling in the bent transition regions and balancing the dispersion of the peak coupling ratio, effective coupling coefficient, and bending phase. One key to balancing the dispersion was the close ~6-μm waveguide separation distance permitted by the femtosecond laser writing technique. The results shown here represent a promising step towards optical engineering of spectral response in femtosecond laser written 3D optical circuits, laying the ground work for designing new devices and optical systems that are not possible with PLC or fiber technologies.

Acknowledgments

The authors gratefully acknowledge the invaluable technical support from Sergey Reznik and helpful insights of Nicolas Godbout. Support from the Canadian Institute for Photonics Innovation and the Natural Sciences and Engineering Research Council of Canada is gratefully acknowledged.

#97770 - $15.00 USD Received 23 Jun 2008; revised 14 Jul 2008; accepted 15 Jul 2008; published 16 Jul 2008